Asymmetric composition profiles in block copolymer interphases: 2. Thermodynamic model predictions and implications

Clayton P. Henderson* and Michael C. Williams†
Chemical Engineering Department, University of California, Berkeley, CA 94720, USA
(Received 14 January 1985)

Evidence for various types of compositional asymmetries associated with the interphase region of microphase-separated block copolymers leads to a classification of four general cases that may exist. The recently modified version of the Leary–Williams thermodynamic model for diblock (AB) and triblock (ABA) copolymers is extended to include all four cases, for planar microstructures. Calculations are performed of free energy and separation temperature corresponding to each case. Results are consistent with experimental observations of interphases found to be rich in the A component, but inconsistent with experiments that indicate residual mixing of B material in the A core. The inference is made that the latter observations correspond to samples that are not in a state of thermodynamic equilibrium.

(Keywords: interphase; block copolymer; asymmetric interphase; microphase separation; copolymer thermodynamics)

INTRODUCTION

Block copolymers are known to form a microheterogeneous structure wherein the two (or more) block components segregate from one another. This microphase separation, illustrated in *Figure 1* for a planar morphology, occurs for diblocks AB, triblocks ABA, and other molecular architectures (ABC, star $(AB)_n$, multiblock ABABAB...). Microstructural parameters of importance are also defined in *Figure 1*: the repeat distance D, the domain sizes T_A and T_B, and the interphase thickness ΔT over which the local composition changes from (mostly) B to (mostly) A. *Figure 2* presents some hypothetical composition profiles which have been used to represent the local volume fraction of component A as a function of distance across the interphase, $\phi'_A(x)$.

The evolution of thermodynamic theory for describing microphase-separated block copolymers has progressed considerably with respect to the incorporation of information about the interphase region in the overall model for the system. The pioneering models of Meier[1] and Krause[2] postulated a sharp interface. The Leary–Williams model[3] was the first to accommodate fully the idea of an interphase region of finite thickness, although it utilized a highly unrealistic step-function composition profile (*Figure 2*) for the sake of mathematical convenience. The later models of Meier[4,5], Helfand[6], and others (see e.g., ref. 7) incorporated more realistic composition profiles. Meier[4,5] acknowledged that some form for a profile must be used (he chose a sinusoidal one), but believed (like Leary–Williams) that the thermodynamic properties were not sensitive to the profile choice. Helfand[6] derived a profile (in the form of a hyberbolic tangent function) based in part on the early work of Cahn and Hilliard[8].

The recent work of Henderson and Williams[9] disputes the idea that properties are insensitive to profile choice by performing calculations for a modified Leary–Williams model for five different composition profiles; ΔT and separation temperature T_s are shown to depend strongly on profile choice as well as on molecular parameters such as total molar volume $\tilde{V}$, volume fractions ϕ_A and ϕ_B of components in the copolymer, and molecular architecture (AB *versus* ABA). In this respect the theories of Meier and Helfand have qualitative and quantitative differences from the Henderson–Williams results. For example, ΔT was calculated as a fixed value independent of $\tilde{V}$ (Helfand), a monotonically decreasing function of $\tilde{V}$ (Meier), or a curve that first increases with $\tilde{V}$, passes through a maximum and then decreases (Henderson–Williams). [These qualitative differences between the theories are not a consequence of the different $\phi'_A(x)$ choices made in each case; such choice affects primarily the magnitude of ΔT.] Direct comparisons of other Henderson–Williams predictions (e.g., $\Delta T(\phi_A)$ or $T_s(\phi_A)$] with those of Helfand and Meier are difficult to make, as graphical presentation of such results are not available for the latter models.

In addition to any inferences about ΔT and $\phi'_A(x)$ that may result from thermodynamic calculations, much recent experimental evidence[10–18] supports the concept[19] that the interphase should play an important role in the rheological and mechanical behaviour of block copolymers. In fact, the rheological behaviour has been proposed[19] as being dependent on details of $\phi'_A(x)$, while the thermodynamic therories are less sensitive to such details because they incorporate only averages involving the profile.

In light of the potential importance of the interphase profile in determining or influencing material properties (morphological, mechanical and rheological), it seems imperative to examine the available experimental evidence concerning the nature of $\phi'_A(x)$. Direct measurement of $\phi'_A(x)$ has not yet proved feasible. However, a recent evaluation[20] of data obtained with a variety of experimental techniques (e.s.r., XPS, d.s.c., viscoelastic properties), used on block copolymer samples of varying architectures

*Currently engaged in postdoctoral work at Stanford University, Department of Chemistry, Stanford, CA 94305, USA.
†To whom correspondence should be addressed.

0032-3861/85/122026-13$03.00

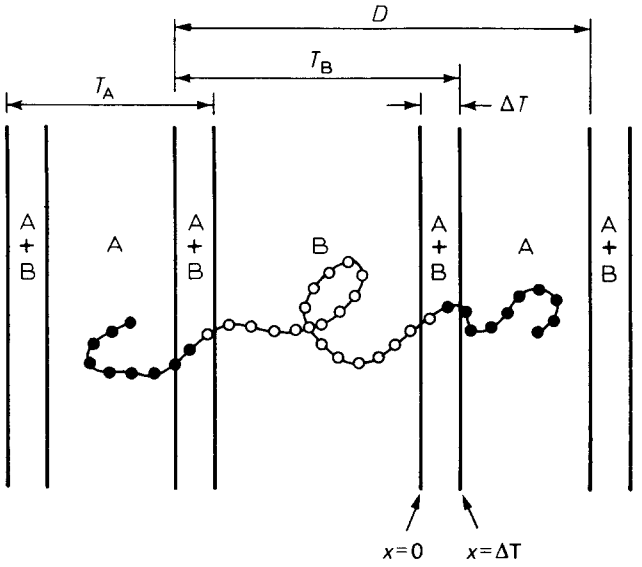

Figure 1 Diagram of microphase-separated block copolymer with planar morphology. Core regions of A and B are separated by an interphase (A + B) of thickness ΔT. A triblock molecule is illustrated, but the relationships between ΔT, the domains sizes T_A and T_B, the core regions, and the planar repeat distance D are defined in the same manner for diblocks

and chemical species, showed that the interphase region is usually rich in one component. (The interphase seems to be consistently rich in the higher-T_g component; if A is the higher-T_g material, then this is equivalent to saying $\overline{\phi'_A} > 0.5$, where $\overline{\phi'_A}$ is the volume average of $\phi'_A(x)$ over $0 \leqslant x \leqslant \Delta T$.) Thus, the interphase profiles in these samples must have been asymmetric.

Unfortunately, these experimentally observed asymmetries are not reflected in the mathematical forms for $\phi'_A(x)$ used by the various thermodynamic theories, all of which have, to date, employed symmetric composition profiles. The question of what effect such asymmetries might have on the thermodynamic predications for block copolymers' properties is therefore unexplored.

The purpose of this paper is to classify the various kinds of asymmetries that might exist, to modify the revised Leary–Williams model[9] to incorporate the possibility of various types of asymmetries, and to present the subsequent thermodynamic predictions for free energy and separation temperature. Results are given primarily for ABA copolymers, and a planar morphology is chosen (following our previous work[9]), in part because the chain statistics are known exactly only in this case.

RESIDUAL MIXING AND CLASSIFICATION OF ASYMMETRIES

Before the thermodynamic model[9] can be altered to accommodate asymmetries, the physical and mathematical nature of the asymmetries must be defined more precisely. There is a considerable body of evidence[20] that $\overline{\phi'_A} > 0.5$, but there are many possible $\phi'_A(x)$ that could account for this physically observed phenomenon. For example, *Figure 2* illustrates several widely different profiles all of which have $\overline{\phi'_A} = 0.50$, and even greater variations could be envisioned for $\overline{\phi'_A} \neq 0.50$.

Another, linked, phenomenon should be considered here: the possibility of residual mixing—or incomplete demixing—in the core region of block domains. Such residual mixing is strongly suggested by experimental evidence, yet this possibility also has not been addressed by thermodynamic models. Before the implications of this mixing are discussed, some of the evidence for its existence will be described.

The most pervasive form of evidence lies in the frequently-observed lowering of the glassy-component T_g (here, T_g^A) in block copolymers relative to T_g of a homopolymer of the same molecular weight. The assumption here is that residual B is dissolved in the predominantly-A microphase lowers T_g^A, just as is observed with 'internally plasticized' random copolymers.

One alternative hypothesis[21] for the observed T_g shift is that of strong 'dynamical interactions' between the two blocks: since the glassy material is connected to a lower-T_g polymer, this connectivity imparts a greater-than-expected degree of molecular motion to at least part of the A chain and hence results in a lower value for the observed T_g^A. However, the inverse argument fails, as an elevation of the T_g^B is rarely if ever encountered. Furthermore, it appears (for polystyrene-containing block copolymers, at least) that the T_g^A decrease depends primarily on the molecular weight of the PS block and not on the chemical nature of the attached 'soft' block[22], as might be anticipated if the 'dynamical interactions' between soft and hard blocks were the primary cause of the T_g^A shift. Ironically, some anomalous data points in the set used to deduce the molecular weight trends in the T_g^A shifts were rationalized[22] on the basis of those samples having a considerable amount of soft material (polyisoprene) mixed within the PS phase.

There have been several attempts[23–25] to predict T_g shifts theoretically as a result of various structural features that might be present in block copolymer systems (cross-links or entanglements; surface-to-volume ratio or other domain-size considerations; mixing in the interphase region). However, these analyses predict T_g shifts which are usually too small to account for the observed cases,

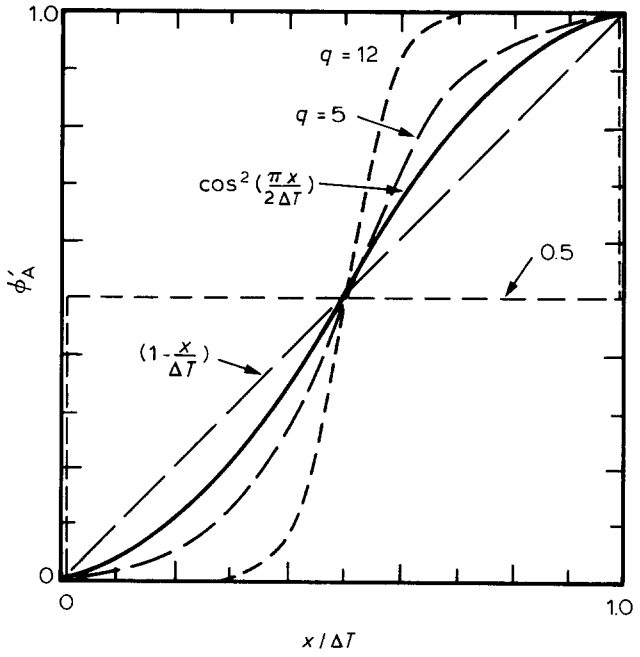

Figure 2 The volume fraction of component A in the interphase plotted as a function of the dimensionless distance across the interphase $x/\Delta T$ for five composition profiles previously used (Step, Linear, Cos^2, Tanh ($q = 5$), and Tanh ($q = 12$)), where q is a shape parameter occurring in the argument of the Tanh profile)

and sometimes are even in the wrong direction. A recent review[26] of block copolymer characterization discussed this issue and concluded that the reason for the abnormal T_g^A decrease is not yet fully understood. The review also emphasizes the importance of the often-neglected factors of copolymer composition and sample treatment, in agreement with the conclusions of our recent thermodynamic work[9].

Nevertheless, several authors[10,27-31] have interpreted the observed T_g shifts to mean that some foreign material was mixed in the core regions. (The core itself is defined to be a homogeneous region, i.e., if there are B chains present in a predominantly A core, they are evenly distributed throughout the core; changes in composition with distance resume only at the core boundary, where the interphase material begins.) Sometimes the observation of a T_g^A shift has led to quantitative estimates of the amount of residual mixing. Zurawski and Sperling[27] estimated 11–16% poly(ethylene-co-butylene) dissolved in the PS phase of a S–EB–S triblock. Diamant *et al.*[10] found 3.5–11% polybutadiene (PB) in the PS phase for SBS triblock copolymers, while Annighofer and Gronski[16] found about 20% PS in the polyisoprene phase of a tapered block copolymer, based on similar arguments and an observed T_g^B shift.

Other authors have used the observed T_g^A shifts to conclude qualitatively (but definitely) that residual mixing exists. For example, d.s.c. results for SB[28] and SBS[28,29] copolymers have led to the inference that some PB must reside in the PS phase. Similar qualitative conclusions have been reached for various block copolymers examined with e.s.r.[30] and n.m.r.[31] (based on T_g^A shifts), and electron microscopy[32]. The last is particularly important conceptually, as direct evidence for mixing was observed (some bromine used to stain the soft component was found in the PS phase). Note that the amount of mixing can be large (e.g., 10% or more) rather than on the trace level of mixing observed[33] in 'incompatible' blends of homopolymers.

If one accepts the possibility of residual mixing in the A phase—and, lacking any other quantitative explanation, this seems the most likely justification for the observed T_g^A shifts—then several consequences arise in regard to the treatment of $\phi'_A(x)$ asymmetries, as the two possibilities (asymmetries and residual mixing) are linked. First, both must be addressed in the mathematical formulation of the model. Secondly, once both phenomena are considered, a synergistic effect reveals itself: the very definition of 'symmetry' depends on the amount of B present in the A core. The complexities of this situation are illustrated in *Figure 3*.

Consider first the simplest case, case I in *Figure 3*: when there is no residual mixing in the A phase (hence $\phi'_A|_{\Delta T} \equiv K = 1.0$) and the profile is symmetric (in the sense that $\overline{\phi'_A} \equiv N = 0.50$). *Figure 3(I)* illustrates two different curve shapes for $\phi'_A(x)$ which meet these criteria, just as *Figure 2* does for several others. All curves in *Figure 2* and *Figure 3(I)* are symmetric visually, that is, $\phi'_A(x/\Delta T = 0.50) = 0.50$ and $\phi'_A(x/\Delta T = 0.50 - \varepsilon) = 1 - \phi'_A(x/\Delta T = 0.50 + \varepsilon)$ for any value ε $(0 \leqslant \varepsilon \leqslant 0.50)$; this results in $N = 0.50$ for all curves.

If the value of K is kept at unity but asymmetries are allowed (i.e., N-values other than 0.50), the resultant curve shapes are obviously asymmetric visually as well

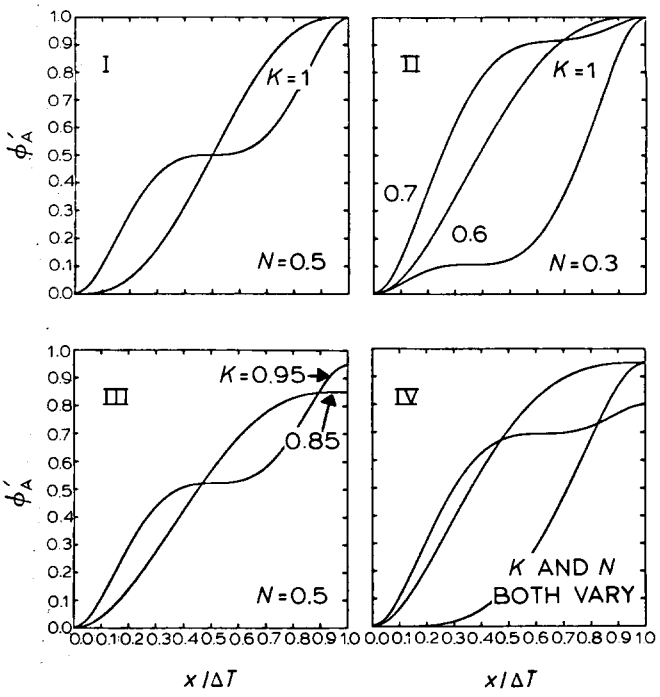

Figure 3 Schematic illustration of possible curve shapes for the interphase composition profile $\phi'_A(x)$. Representative $\phi'_A(x)$ are plotted as a function of dimensionless distance across the interphase for each of the four possibilities resulting from combinations of $\{N = 0.5, N \neq 0.5\}$ and $\{K = 1, K \neq 1\}$, where $N \equiv \overline{\phi'_A}$ is the volume-averaged fraction of component A in the interphase, and $K \equiv \phi'_A(x/\Delta T = 1)$ is the volume fraction of component A in the A core region. Case I is symmetric ($N = 0.5$, $K = 1$), case II has $K = 1$ but allows N to vary, case III is the reverse of that, and case IV allows both to vary ($N \neq 0.5$, $K \neq 1$)

$[\phi'_A(x/\Delta T = 0.50 - \varepsilon) \neq 1 - \phi'_A(x/\Delta T = 0.50 + \varepsilon)]$ and the two criteria agree. *Figure 3(II)* displays profiles with K values of 0.30 (rich in B), 0.60, and 0.70 (rich in A) to illustrate this case.

But once one allows mixing in the A phase, then $K < 1.0$ and the two criteria are no longer equivalent. Consider *Figure 3(III)*: both curves there are obviously asymmetric visually $[\phi'_A(x/\Delta T = 0.50 - \varepsilon) \neq 1 - \phi'_A(x/\Delta T = 0.50 + \varepsilon)]$ yet both have $N = 0.50$ and are 'symmetric' in that sense. It should be noted that cases I and III in *Figure 3* would both result in experimental values for N that imply symmetry, even though case III is not symmetric visually.

Finally, case IV in *Figure 3* displays several profiles for which $N \neq 0.50$ and $K \neq 1.0$. One profile, corresponding to $K = 0.95$, has a value $N = 0.60$ just as one of the curves in case II does, albeit with $K = 1.0$. Thus, an experimental observation of $N = 0.60$ could not distinguish between these curve shapes, just as knowledge that $N = 0.50$ would be insufficient to allow a choice between any $\phi'_A(x)$ in *Figure 2* or *Figure 3(I)*.

The four cases exhibited in *Figure 3* correspond to all possible combinations of $\{K = 1, K \neq 1\}$ and $\{N = 0.50, N \neq 0.50\}$. In terms of the thermodynamic model being used here[9], no adjustments to the theory are required to make predictions for cases I and II (i.e., for $K = 1$, or no residual mixing); only a knowledge of $\phi'_A(x)$ is required. 'Indeed, all previous[9] work falls in case I.) However, considerable modification is necessary to account for the physical changes that accompany the intermingling of B chains in the A core as occurs in cases III and IV.

EXTENSION OF THE THERMODYNAMIC THEORY

Summary of the existing model

The model employed here to examine the effect of asymmetries and residual mixing is the recently modified version[9] of the Leary–Williams thermodynamic theory[3]. Previous publications[3,9] present derivations and explanations of the model features in great detail and only a brief summary is given here to enable the reader to evaluate subsequent additions.

Certain material balance relationships, valid for the case where $K = 1$ (no residual mixing), arise immediately from the definitions illustrated in *Figure 1* for planar morphology. The volume fraction of interphase material is given by

$$f = 2\Delta T/D = 2\beta\phi_A/(1 - 2\beta\overline{\phi'_B}) \tag{1}$$

where β is the dimensionless interphase thickness

$$\beta \equiv \Delta T/T_A \tag{2}$$

and $\overline{\phi'_B} = 1 - \overline{\phi'_A}$. The formal definition of $\overline{\phi'_A}$ and $\overline{\phi'_B}$ is given by

$$\overline{\phi'_A} = 1 - \overline{\phi'_B} = \frac{1}{\Delta T}\int_0^{\Delta T} \phi'_A(x)\mathrm{d}x \tag{3}$$

Other morphological relationships (e.g., for D or T_B) are available but are not needed here.

The general approach is to write an expression for the Gibbs free energy difference between the postulated structured (microphase-separated) system and the corresponding homogeneous reference system at the same temperature:

$$\Delta G = G_{struc} - G_{homog} = \Delta H - T\Delta S \tag{4}$$

The enthalpic term is evaluated from a knowledge of the morphology via

$$\Delta H = -\Delta H_{mix} = -\tilde{V}(\delta_A - \delta_B)^2[\phi_A\phi_B - f\overline{\phi'_A\phi'_B}] \tag{5}$$

Here $\tilde{V}$ is the total molar volume, δ_A and δ_B are the solubility parameters, and $\overline{\phi'_A\phi'_B}$ is

$$\overline{\phi'_A\phi'_B} = \frac{1}{\Delta T}\int_0^{\Delta T} \phi'_A(x)\phi'_B(x)\mathrm{d}x \tag{6}$$

The extra term involving f in equation (5) subtracts off the contribution from the interphase—where there is still mixing of A and B.

The entropic terms, which depend on molecular architecture (AB *versus* ABA), consist of three contributions:

$$\Delta S = \Delta S_1 + \Delta S_A + \Delta S_B \tag{7}$$

Here, ΔS_1 results from confining the block junction to the interphase region while the ΔS_i (with i = A or B) represent the entropy change, relative to the homogeneous case, in restricting the i block to reside only in the T_i region, where T_i is the thickness of the pure-i core plus the adjacent interphase regions. Simple probability arguments[3,9] lead readily to

diblocks $$\Delta S_1^{di} = R\ln(f) \tag{8a}$$

triblocks $$\Delta S_1^{tri} = R\ln(2f - f^2) \tag{8b}$$

where R is the gas constant.

The origins of ΔS_i expressions are considerably more complicated, involving solutions for chain probabilities or distribution functions, and will not be described here. The major difference between the ΔS_i for diblocks and triblocks is that in the diblock case both chains in the copolymer molecule have one end free and one end (the AB junction) confined to an interphase, while in the triblock case the A and B blocks are topologically different (A is as before, but the middle B block has both ends restricted to interphase regions). For diblocks, therefore, both ΔS_A and ΔS_B have the form

$$\Delta S_i^{di} = R\ln(P_i) - (3R/2)[\alpha_i^2 - 1 - \ln(\alpha_i^2)] \tag{9}$$

Here α_1 is the chain expansion parameter

$$\alpha_i^2 = \langle r_i^2\rangle / \langle r_i^2\rangle_0 \tag{10}$$

which measures the perturbation of the block coil size from the end-to-end distance of the corresponding homopolymer. The complete expression for the probability P_i in equation (9) is given in ref. 9. For triblocks, the ΔS_A^{tri} term has the form of equation (9) but is multiplied by 2 since both A blocks contribute; the B block is represented by

$$\Delta S_B^{tri} = R\ln(P_B) - (3R/2)[\alpha_B^2 - 1] \tag{11}$$

The terms involving the α_i in equations (9) and (11) are elastic entropy contributions (since in general $\alpha_i \neq 1.0$) and are evaluated primarily through a knowledge of a second model parameter Γ, the dimensionless domain size

$$\Gamma \equiv T_A^2/\langle r_A^2\rangle \tag{12}$$

which can be related to α_A^2 and α_B^2.

The minimum free energy ΔG_{min} is found by varying β and Γ; in practice this requires an assumption about the nature of $\phi'_A(x)$ in order to calculate values for $\overline{\phi'_B}$ and $\overline{\phi'_A\phi'_B}$. All other parameters are known once a given block copolymer is specified (ϕ_A, $\tilde{V}$, δ_A and δ_B, homopolymer physical properties). Once ΔG_{min} is obtained, morphological properties (e.g., the magnitude of ΔT or D) can be found from knowledge of β_{min} and Γ_{min}. If $\Delta G_{min} < 0$, the equilibrium morphology is microphase-separated with values of D, T_A, T_B and ΔT as calculated from β_{min} and Γ_{min}. If $\Delta G_{min} > 0$ the equilibrium morphology at that temperature is homogeneous and any morphological calculations correspond only to a fictitious state. The separation temperature T_s occurs when $\Delta G = 0$ and is found through a similar procedure whereby one searches for the maximum value of $T_s(\beta, \Gamma)$, which generally does not correspond exactly to the microstructure characterized by β_{min}, Γ_{min} at any fixed temperature.

Alterations allowing residual mixing

Defining the volume fraction of A in the A core as K (and hence $1-K$ = volume fraction of residual B in the A core) leads to several material balance relationships[34]:

$$f = 2\beta\phi_A/\{K + 2\beta[\overline{\phi'_A} - \phi_A - K(1-\phi_A)]\} \quad (13a)$$

$$T_B/T_A = (K-\phi_A)/\phi_A + \frac{2\beta}{\phi_A}\{\overline{\phi'_A} - K(1-\phi_A)\} \quad (13b)$$

$$f_{AC} = \phi_A(1-2\beta)/\{K + 2\beta[\overline{\phi'_A} - \phi_A - K(1-\phi_A)]\} \quad (13c)$$

Here f_{AC} is the volume fraction of the A core region (the thickness of the core is just $T_A - 2\Delta T$) and all other symbols are the same as previously defined. It is readily apparent that if $K=1$ (no residual mixing) then equation (13a) reduces to the previous result for f, equation (1). Similarly, the relationship for T_B can be shown to reduce to the earlier one[9] when $K=1$. If D is needed it can be obtained from

$$D = T_A[1 + T_B/T_A - 2\beta] \quad (14)$$

and ΔT and T_A are calculated exactly as in the $K=1$ case[9]. The above relationships assume that the B core is pure B material; if this assumption were to be relaxed, then analogous relationships could readily be derived.

The enthalpic contribution is conveniently given in terms of $\Delta H^{(1)}$, defined by equation (5) for the $K=1$ case:

$$\Delta H = \Delta H^{(1)} + f_{AC}K(1-K)\tilde{V}(\delta_A - \delta_B)^2 \quad (15)$$

Here the new term is analogous to the interphase contribution in the original expression: it accounts for material that is still partially mixed.

In order to evaluate the entropic effects of residual mixing, a new parameter is needed; let ψ be defined as the fraction of AB junctions which reside in the A core (instead of in the interphase region as before). Since the number of B blocks is strictly proportional to the number of B junctions (one of each in diblocks, two of each in triblocks), ψ also equals the volume fraction of all B chains that are in the A core (instead of in the T_B region as before). This argument neglects those cases where part of a B chain is outside the A core region even though the AB junction is not; the number of such configurations present (and of the corresponding case for A chains) is expected to be extremely small. The reasons for this will be discussed in more detail in the Appendix.

Once ψ is equated with the fraction of all B chains which are located in the A core, material balance considerations can be used to derive a relationship between ψ and other parameters. For example, $\psi(K)$ is given by

$$\psi = \left(\frac{\phi_A}{1-\phi_A}\right)\left(\frac{1-K}{K}\right)(1 - f\overline{\phi'_A}) \quad (16)$$

A knowledge of ψ allows stipulation of the form of the equations for the new entropy terms, as described below.

There are now two kinds of A chains: 'old' (one end in the interphase, tied to the junction there), and 'new' (located entirely within the A core and connected to a junction which is itself inside the core region). Similarly, there are now two kinds of B chains; the 'old' B chains have one or both ends—depending on molecular architecture, AB *versus* ABA—in the interphase with the rest of the block distributed throughout the B domain, while the 'new' B chains have one or two junctions (depending on architecture, but always all junctions) in the A core region, along with the attached A chain(s).

Let $\Delta S_1^{(1)}$, $\Delta S_A^{(1)}$ and $\Delta S_B^{(1)}$ be the previously defined expressions for the entropy terms associated with the chains in the 'old', or $K=1$, positions as described above [equations (8), (9) and (11)]. Let $\Delta S_1^{(K)}$, $\Delta S_A^{(K)}$ and $\Delta S_B^{(K)}$ be associated with chains which, in the microphase-separated system, find themselves in the 'new' positions. By definition, the fraction of A chains, B chains and junctions that are in the 'old' configuration is just $1-\psi$, while the fraction in the 'new' positions is ψ. Hence one can write

$$\Delta S_1 = (1-\psi)\Delta S_1^{(1)} + \psi\Delta S_1^{(K)} \quad (17a)$$

$$\Delta S_A = (1-\psi)\Delta S_A^{(1)} + \psi\Delta S_A^{(K)} \quad (17b)$$

$$\Delta S_B = (1-\psi)\Delta S_B^{(1)} + \psi\Delta S_B^{(K)} \quad (17c)$$

It can further be argued that, since the 'new' A and B chains are free to wander randomly within the A core region—their junctions are not restricted to the interphase, nor do other constraints apply to them as they do to the 'old' chains[9]—then the configurations of these chains should not be much perturbed from the random coil configuration of the homogeneous melt. Therefore, to a good first approximation, $\Delta S_A^{(K)} = \Delta S_B^{(K)} = 0$.

The $\Delta S_1^{(K)}$ term is not zero, however, and it must be evaluated for the two cases of diblock and triblock architectures. $\Delta S_1^{(K)}$ represents the entropy change associated with restricting the junctions of the 'new' type copolymer molecules to lie in the A core rather than being distributed randomly throughout all space (as in the homogeneous reference state). For diblocks this term has the same form as $\Delta S_1^{(1)}$, except that f, the volume fraction of the interphase (where the 'old' junction is confined), is replaced with f_{AC}, the volume fraction of the A core (where the 'new' junction resides):

$$\text{diblocks} \qquad \Delta S_1^{(K),di} = R\ln(f_{AC}) \quad (18)$$

For triblocks the relationship is not the same any longer, and the form of ΔS_1 changes. The term $\Delta S_1^{(1)}$ for triblocks represents the entropy change associated with placing at least one junction in an interphase; the placement of the second junction is accounted for in the $\Delta S_B^{(1)}$ term for triblocks (details[9] involve the generation of the probability term P_B). For the 'new' triblock chains, though, there is only the A core region in which both junctions wander randomly and continuously—there is no second region to be accommodated as in the 'old' case (where the second junction also had to be placed in an interphase region, either the same one or an adjacent one). Hence for the 'new' triblock case the probability of having the first junction randomly position itself in the A core is just f_{AC}, the probability of the second junction doing so is the same, and the probability of both junctions randomly situating themselves in the A core is f_{AC}^2. Therefore,

$$\text{triblocks} \qquad \Delta S_1^{(K),tri} = R\ln(f_{AC}^2) \quad (19)$$

The new case when $K=1$ is now completely defined for the purposes of making calculations, as soon as the value

of K is specified and the profile details needed to calculate $\overline{\phi'_A}$ and $\overline{\phi'_A\phi'_B}$ are provided. Knowledge of K gives ψ via equation (16) and allows the calculation of the material balance relationships [equation (13)] and, from there, the enthalpic [equation (15)] and entropic [equations (17)–(19)] contributions to ΔG. The free energy is minimized with respect to β and Γ just as before for any combination $\{K, \overline{\phi'_A}, \overline{\phi'_A\phi'_B}\}$. In a sense these three parameters all constitute profile information; if there is residual B in the A core, then $\phi'_A|_{x=\Delta T} \equiv K$ gives $K<1$ instead of unity. Thus, K, $\overline{\phi'_A}$ and $\overline{\phi'_A\phi'_B}$ are interrelated, and all reflect the assumed form for the interphase composition profile.

CALCULATIONS

Profile choice

It is desirable to have a single mathematical form for $\phi'_A(x)$ which would encompass all four cases illustrated in *Figure 3*. A general fifth-order polynomial form was chosen as convenient:

$$\phi'_A(x) = C_0 + C_1(x/\Delta T) + a(x/\Delta T)^2 + b(x/\Delta T)^3 + c(x/\Delta T)^4 + d(x/\Delta T)^5 \quad (20)$$

Then, with the four boundary conditions $\phi'_A|_{x=0} = 0$, $\left.\frac{d\phi'_A}{dx}\right|_{x=0} = 0$, $\phi'_A|_{x=\Delta T} = K$, $\left.\frac{d\phi'_A}{dx}\right|_{x=\Delta T} = 0$, and the definition $\overline{\phi'_A} = N$, there results $C_0 = C_1 = 0$ and

$$a = 3K + 15(2N - K) - d/2 \quad (21a)$$

$$b = -2K - 30(2N - K) + 2d \quad (21b)$$

$$c = 15(2N - K) - 5d/2 \quad (21c)$$

Thus $\phi'_A(x)$ is completely defined in terms of the physically meaningful variables K and N (or $\overline{\phi'_A}$), and the adjustable parameter d. The latter will be referred to as the 'shape' parameter, as the profile shape (and hence $\overline{\phi'_A\phi'_B}$) depends on d:

$$\overline{\phi'_A\phi'_B} = a/3 + b/4 + (c - a^2)/5 + (d - 2ab)/6 - (b^2 + 2ac)/7 - (ad + bc)/4 - (c^2 + 2bd)/9 - cd/5 - d^2/11 \quad (22)$$

where the coefficients a, b and c are defined above in terms of d.

There are other constraints on $\phi'_A(x)$ that limit the admissible values of d: $\phi'_A(x)$ and $\phi'_B(x)$ are always between 0 and 1 individually, and $\phi'_A(x)$ should be a monotonically increasing function of x (on physical grounds). Together, these constraints dictate a different acceptable range of d values for each combination of N and K chosen. For example, for $N = 0.50$ and $K = 1.0$, the acceptable range is $-24 \leqslant d \leqslant +6$. As K deviates more severely from unity, the range of d becomes more confined.

Figure 4 shows the behaviour of $\overline{\phi'_A\phi'_B}$ as a function of d, and parametrically of K, for N fixed at 0.50. (Similar behaviour is seen for other values of N, or for $\overline{\phi'_A\phi'_B}$ as a function of d and N at fixed K.) The envelope in *Figure 4* bounds the region of acceptable d values. The bottom curve for $K = 1.0$ is useful when comparing to previous case I profiles. For example, the case I profiles ($N = 0.50$, $K = 1.0$) in *Figure 2* have $\overline{\phi'_A\phi'_B}$ values ranging from 0.2500 (the unrealistic Step function) to 0.04167 (Tanh profile with $q = 12$). By comparison, a polynomial profile with $N = 0.50$, $K = 1.0$ produces a $\overline{\phi'_A\phi'_B}$ range from 0.1840 ($d = -24$) to 0.1082 ($d = 6$), and the choice $d = 1.0$ has $\overline{\phi'_A\phi'_B} = 0.1254$, which very closely mimics the $\cos^2$ profile ($\overline{\phi'_A\phi'_B} = 0.1250$) in *Figure 2*. Qualitatively, the value of $\overline{\phi'_A\phi'_B}$ is a rough measure of the 'sharpness' of the profile, especially in the ascending region.

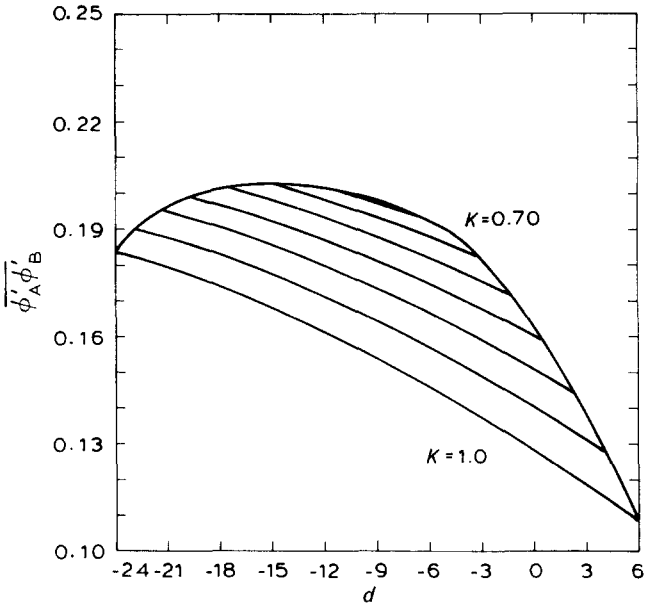

Figure 4 Values of $\overline{\phi'_A\phi'_B}$ as a function of the shape factor d for the polynomial profile defined by equation (20); each curve terminates at the upper and lower values of d permitted by the various constraints imposed on profile shape. Here $N = 0.5$, and the K dependence is illustrated parametrically in the envelope of curves: the $K = 1$ limit corresponds to case I illustrated in *Figure 3*, while all other curves would fall under case III. Curves are displayed corresponding to increments of 0.05 in K, ranging from $K = 1$ (bottom) to $K = 0.70$ (top)

Table 1 Details of profiles displayed in *Figure 3*

Case	Curve	K	N	d	$\overline{\phi'_A\phi'_B}$
I	1	1	0.50	6	0.10823
I	2	1	0.50	−24	0.18398
II	1	1	0.30	−17.5	0.11595
II	2	1	0.60	0	0.11429
II	3	1	0.70	−15	0.11131
III	1	0.85	0.50	1	0.15713
III	2	0.95	0.50	−22.5	0.19017
IV	1	0.95	0.30	−5	0.10146
IV	2	0.95	0.60	−2	0.12959
IV	3	0.80	0.55	−14.5	0.18956

All of the profiles used in *Figure 3* to illustrate the four cases were actually generated using the polynomial profile developed above. *Table 1* lists the values of $\{N, K, d$ and $\overline{\phi'_A\phi'_B}\}$ associated with each of the $\phi'_A(x)$ displayed in *Figure 3*. Note that curves 1 and 2 in case II have values for $\overline{\phi'_A\phi'_B}$ that are almost identical, yet at the same time possess N values that are extremely far apart (0.30 and 0.60). This emphasizes how important it is to characterize the interphase composition profile by more than one parameter.

Physical properties used in calculations

All physical property parameters for the A and B blocks were chosen to correspond to polystyrene (for A) and polybutadiene (for B). Values used for densities were $\rho_A = 1.05$ g cm^{-3}, $\rho_B = 0.97$ g cm^{-3}, for the Kuhn parameter (relating molecular weight and hompolymer end-to-end distance) $K_A = 0.067$ nm (0.67 Å), $K_B = 0.086$ nm (0.86 Å), and for solubility parameter difference $\delta_A - \delta_B = 1.64$ (J m^{-3})$^{1/2}$ or 0.80 (cal cm^{-3})$^{1/2}$. Discussion of these values is provided elsewhere[9], but for the present purposes the magnitudes of the ρ_i, K_i and δ_i do not matter as much as the fact that their values are fixed. The calculations here will be for AB and ABA architectures, with $\tilde{V} = 100\,000$ cm^3 gmole^{-1} and composition either fixed (at $\phi_A = 0.50$) or varied from $\phi_A = 0.1$ to $\phi_A = 0.90$. The calculations are intended to investigate the effect of profile asymmetries, including the possibility of residual mixing, and therefore the profile parameters N, K and d are treated here as the primary variables.

MODEL PREDICTIONS

Previous publications[3,9] have described in great detail the process for finding $\Delta G_{min}(\beta,\Gamma)$, the model dependencies on β, Γ and copolymer properties, and the values of morphological properties such as ΔT or D. Here the emphasis is on evaluating which of several possible interphase profile shapes is thermodynamically preferred, usually for a fixed block copolymer molecule. The effects of molecular weight (or molar volume), copolymer composition, chemical difference and molecular architecture (AB *versus* ABA) are the same as reported before and for the most part will not be reiterated here.

Calculations for the various profiles of case I through case IV were performed on a $\{\beta,\Gamma\}$ grid at intervals of 0.05, and hence the values of β_{min} and Γ_{min} are accurate to ± 0.025 at best. This leads to a slight roughness in some figures, but all general trends are unambiguous and qualitative conclusions should not be altered by finer-grid results. Most Γ_{min} values are on the order of 1–2 and β_{min} is on the order of 0.20–0.25 for the $\tilde{V} = 10^5$ cm^3 gmole^{-1}, $\phi_A = 0.50$ copolymer employed most frequently in the calculations.

Case I results

This case is really symmetric, as was so in our earlier work[9], so no case I results will be presented separately here. Because calculations actually employ $\overline{\phi'_A}$ and $\overline{\phi'_A\phi'_B}$ rather than the details of $\phi'_A(x)$, any case I (polynomial profile (with $\overline{\phi'_A} = 0.50$, by definition) will result in calculated properties that are identical to any previous results[9] for a symmetric profile with the same value of $\overline{\phi'_A\phi'_B}$. For example, all calculations for the sinusoidal profile apply (for practical purposes) to the $\{d = 1,\ N = 0.50,\ K = 1.0\}$ polynomial profile, since their values of $\overline{\phi'_A\phi'_B}$ are so close. Because $\overline{\phi'_A\phi'_B} = 0.2500$ for the Step function and 0.09866 for the $q = 5$ Tanh profile (used extensively before[9]) serve as upper and lower bounds for the polynomial profile values, the polynomial profile predictions are also bounded by the Step and $q = 5$ Tanh predictions. In subsequent presentations of results for cases II–IV, some case I results will be included for comparison, and as limiting cases (e.g., case I is a limiting case for case II as $\overline{\phi'_A}$ or $N \rightarrow 0.50$ and for case III as $K \rightarrow 1.0$).

Case II results

Here there is no B in the A core ($K = 1$) and only shape asymmetries ($N \neq 0.50$) are allowed. *Figure 5* presents ΔG_{min} calculations for a set of case II polynomial profiles for an ABA copolymer with $\phi_A = 0.50$. The temperature is 373 K, approximately the T_g of PS. An envelope, showing the allowable range of $\{N,d\}$ values for the polynomial profile, is defined by two curves. The upper curve (for higher ΔG_{min} values) corresponds to the smallest permissible value of d, while the lower curve (for the lower ΔG_{min} values) represents the large-d limit, for a given value of N. At any fixed value of N, the vertical distance through the envelope in *Figure 5* represents the variation in properties (here, ΔG_{min}) that can be obtained by varying the shape factor.

Two qualitative results are indicated by *Figure 5*. First, for any fixed N the higher d values result in lower ΔG_{min}, which implies that higher-d profiles would be preferred to lower-d ones. (See *Figure 3* and *Table 1* for what this means in terms of the actual shape of $\phi'_A(x)$.) This observation is in qualitative agreement with previous results[9] based on varying $\overline{\phi'_A\phi'_B}$ for fixed $\overline{\phi'_A} = 0.50$. Secondly, there is no true or global minimum ΔG^*_{min} displayed; instead, $\Delta G_{min}(N,d)$ decreases continuously with increasing N until the highest permissible N value (about 0.73) is reached. Beyond that limit, no set of parameters can be found which allows the polynomial profile to obey the various constraints imposed upon it.

All of the calculations displayed in *Figure 5* are for 373 K. Results for $\Delta G_{min}(N,d)$ at 298 K are very similar to *Figure 5* and will not be displayed here; the main effect of the temperature difference is a slight shifting of the magnitude of ΔG_{min} ($\Delta G^{298}_{min} < \Delta G^{373}_{min}$ for N and d constant, as expected, since 298 K is further below the separation temperature than 373 K).

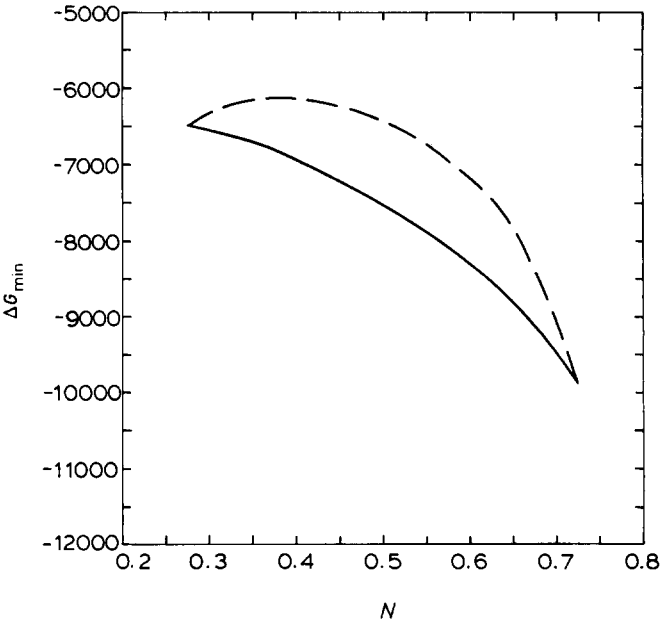

Figure 5 Values for the minimum free energy ΔG_{min} at 373 K for an SBS triblock with $\tilde{V} = 10^5$ cm^3 gmole^{-1}, $\phi_A = 0.50$, and $\delta_A = \delta_B = 1.6$ (J m^{-3})$^{1/2}$ or 0.80 (cal cm^{-3})$^{1/2}$; all calculations are for the polynomial profile with $K = 1$. The N-dependency of ΔG_{min} is illustrated directly, and the d-dependency is illustrated by the upper and lower bounds of the envelope (the vertical range in ΔG_{min} corresponds to the possible variation with shape factor d for fixed N, with the lowest value of ΔG_{min} resulting from the highest value of d)

Values for $T_s(N)$ were also obtained for the same block copolymer and are presented in *Figure 6*. Again, parametric dependence on d is shown, and the envelope of T_s values corresponds to the acceptable range in d for each value of N. Now the high-d side of the envelope is that with greater values of T_s, and the low-d side is associated with smaller T_s magnitudes. This is not a reversal from the behaviour in *Figure 5*, as in both cases the 'high-d' limit is thermodynamically preferred. At a fixed temperature the lowest free energy is preferred (see *Figure 5*), but when the temperature is allowed to change (see *Figure 6*) the structure associated with the highest T_s will form first upon cooling and is therefore preferred. (By definition, $\Delta G = 0$ at T_s for each structure; therefore, above the T_s for a given structure—or profile in this case— $\Delta G > 0$ for that structure, and any other structure with a higher T_s will be preferred to the first.) *Figure 6* also shows the same qualitative N-dependency as in *Figure 5*: the thermodynamically favoured profile turns out to be on the high-N edge of the allowable profiles, with $T_s(N)$ an increasing function. Again the maximum (analogous to the minimum in *Figure 5*) is on the edge of the range explored and any conclusions must be tempered by a recognition of that fact. Nonetheless $N \equiv \overline{\phi'_A} > 0.50$ values seem to be preferred to $\overline{\phi'_A} = 0.50$, in agreement with experimental observations.

Figure 7 displays the dependence of T_s on copolymer composition for ABA copolymers with $N = 0.40$ and $N = 0.60$. The envelopes correspond to the range of permissible d values as before, with $d_{max} - d_{min}$ relationships for each N identical to that of *Figure 6* (i.e., T_s is greater for d_{max} in each set of curves on *Figure 7*). Results for $\overline{\phi'_A} = 0.50$, not displayed in order to avoid crowding the Figure, lie in between the $N = 0.40$ and $N = 0.60$ cases, as expected. It should be noted that T_s is not symmetric about $\phi_A = 0.50$ for $\overline{\phi'_A} = 0.40$ and 0.60, in agreement with previous observations for the $\overline{\phi'_A} = 0.50$ case (e.g., for case I profiles).

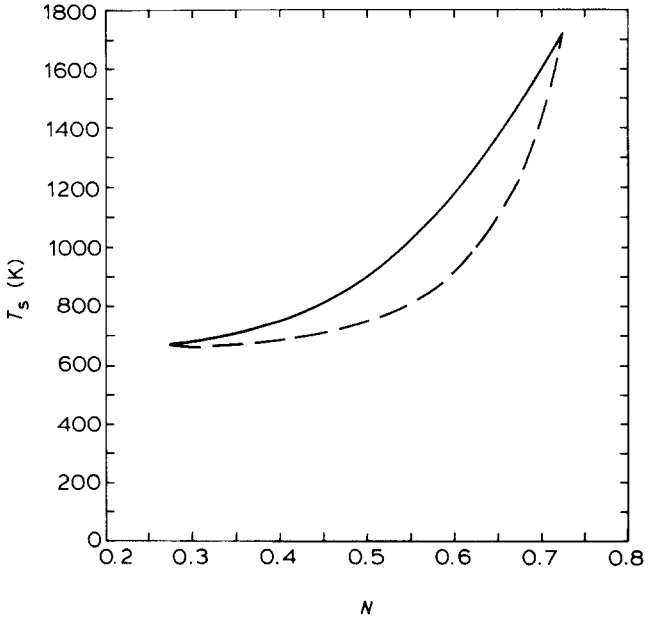

Figure 6 The separation temperature T_s is illustrated as a function of N (directly) and d (parametrically) for the same SBS triblock as in *Figure 5*. Again $K = 1$, and the vertical distance in T_s values, for N fixed, represents the effect of the shape factor, with the upper curve corresponding to the largest permissible value of d

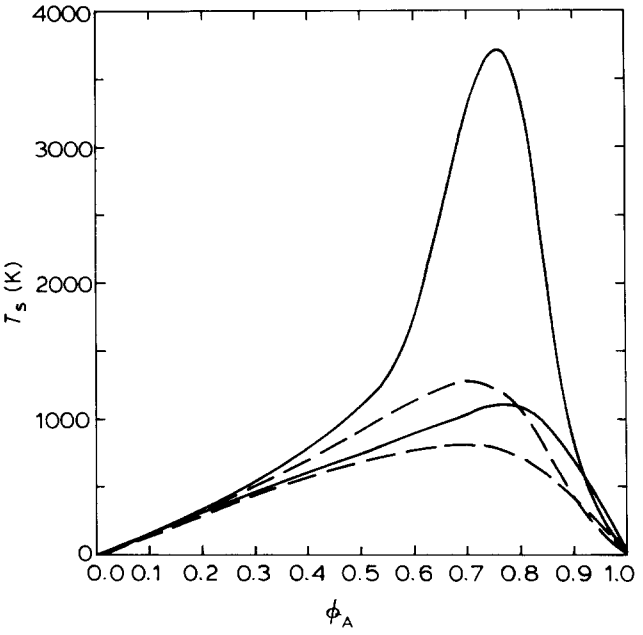

Figure 7 The copolymer composition dependency of the separation temperature $T_s(\phi_A)$ is illustrated for $K = 1$ and two values of N: the upper envelope of T_s values is for $N = 0.60$, and the lower envelope corresponds to $N = 0.40$. Results are for an SBS triblock with $\tilde{V} = 10^5$ cm^3 gmole^{-1}, $\delta_A - \delta_B = 1.6$ (J m^{-3})$^{1/2}$, or 0.80 (cal cm^{-3})$^{1/2}$, and with composition varying as indicated in the Figure. In each envelope the highest value for T_s corresponds to the highest allowable value for d, and the vertical range within the envelope represents the effect of varying d, for fixed composition ϕ_A. The top solid and broken lines are for $N = 0.6$, and the lower lines for $N = 0.4$

The molecular weight dependencies of ΔG_{min} and T_s will not be displayed, as the alterations here in profile choice do not strongly affect them; T_s is almost exactly proportional to $\tilde{V}$, and $\Delta G_{min}(\tilde{V})$ for fixed temperatures decreases continuously, as previously reported[9] for case I profiles. (Note that case I results are presented in *Figures 5* and *6* if one examines the vertical slice corresponding to $\overline{\phi'_A} = 0.50$.)

Case III results

In this case $\overline{\phi'_A} = 0.50$ but $K < 1.0$. *Figure 8* displays the copolymer composition influence on ΔG_{min} at 373 K for a residual mixing level of $K = 0.95$ (5% B in the A core) and, as a reference, for the case I limit of $K = 1$. The d-range envelope for the case with residual mixing is always above ΔG_{min} values for case I results, implying that such mixing is not thermodynamically favoured in the bulk state if $\overline{\phi'_A} = 0.50$. Also, $\Delta G_{min}(\phi_A)$ is not symmetric about $\phi_A = \phi_B = 0.50$ for either K value.

Figure 9 examines the effect of varying the K value. ΔG_{min} at 373 K is presented for both architectures (AB and ABA) with $N = 0.50$. Copolymer composition and molar volume are fixed for both AB and ABA molecules at $\phi_A = 0.50$ and $\tilde{V} = 10^5$ cm^3 gmole^{-1}. The architectural dependence of ΔG_{min} is exactly as would be anticipated based on case I results[9] ($K = 1.0$ in *Figure 9*), with the diblock being consistently more stable, having a lower ΔG_{min} than the triblock at a fixed temperature. Note that the $\Delta G_{min}(K,d)$ envelopes show qualitatively identical results for both architectures: ΔG_{min} decreases continuously as K increases, reaching a lower bound at $K = 1$. Therefore the thermodynamically favoured case is, indeed, the $K = 1$ case in *Figure 9*.

Figure 10 results in similar conclusions when the $T_s(K,d)$ behaviour is examined. Therefore, if the profile average is

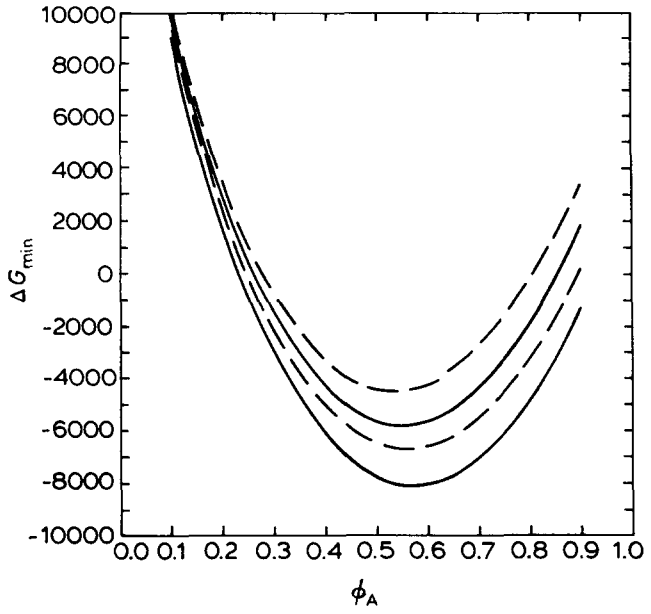

Figure 8 The copolymer composition dependence of the minimum free energy $\Delta G_{min}(\phi_A)$ at 373 K is exhibited for the same SBS triblocks used in *Figure 7*. Here N is fixed at 0.50, and two sets of curves are presented as a function of K: the upper envelope, for higher ΔG_{min} values, is for $K = 0.95$, while the lower envelope is for $K = 1$ (case I). Again, variation in shape factor accounts for there being an envelope of curves, with the lowest value of ΔG_{min} in each envelope corresponding to the highest allowable d. The top two lines are for $K = 0.95$, and the bottom two for $K = 1$

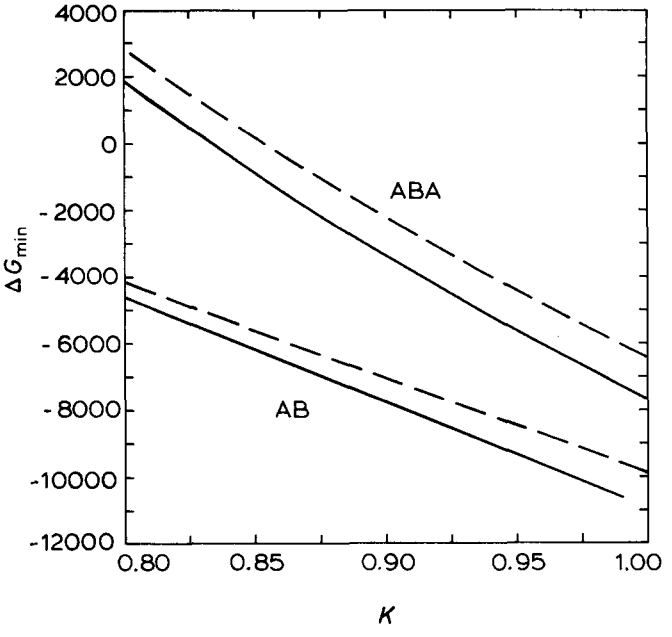

Figure 9 Diblock and triblock results (A = PS, B = PB) for the variation in ΔG_{min} with K. Here N is fixed at 0.50, and both diblock and triblock have the same values for $\tilde{V}$ (10^5 cm^3 gmole^{-1}), $\phi_A(0.50)$, and $\delta_A - \delta_B = 1.6$ (J m^{-3})$^{1/2}$ = 0.80 {cal cm^{-3}}$^{1/2}$. For each architecture, the highest value of ΔG_{min} is for the lowest value of shape factor, and the lowest value of ΔG_{min} illustrated is for the highest d value. Results for the case I symmetric limit are found at edge of the Figure where $K = 1$

$\overline{\phi'_A} \equiv N = 0.50$, the preferred morphology should not contain any residual mixing in the A core.

Case IV results

By allowing both K and N to vary continuously, the possibility of finding an overall preferred state can be examined. Graphical presentations cannot accommodate the effects of all independent variables simultaneously, so we shall illustrate major trends by choosing selected cases for display.

Figures 11 and *12* present calculations for ΔG_{min}^{373} and T_s (for a triblock with $\phi_A = 0.50$) as a function of N, but only for $K = 0.95$. Results qualitatively similar to the $K = 1$ case (*Figure 5* and *6*) are observed, i.e. the lowest ΔG_{min} and highest T_s occur at the high-N boundary of the envelope of acceptable polynomial profiles. Thus, for case IV too, interphases rich in the high-T_g component seem to be favoured.

Another 'slice' through the $\Delta G_{min}(N,K)$ function is illustrated in *Figure 13* for $N = 0.60$ and K varying. This bears a great resemblance to the $N = 0.50$ variation with K

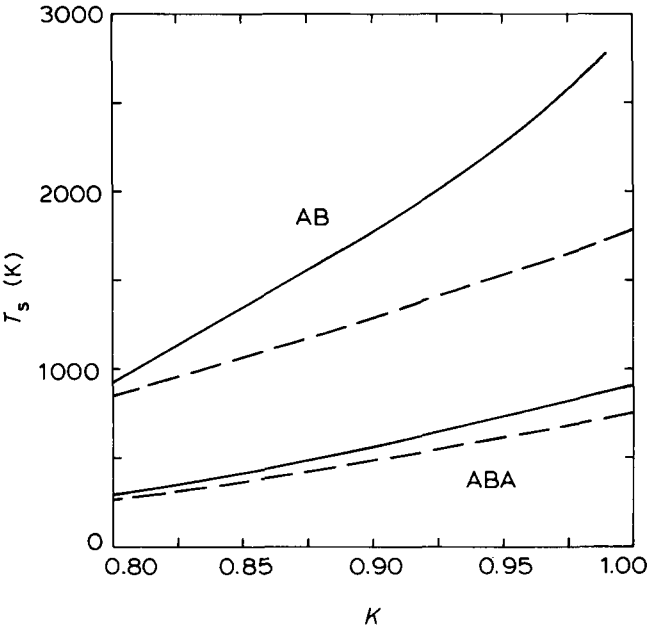

Figure 10 Results for $T_s(K)$ are displayed for the same SB and SBS copolymers as in *Figure 9*. Here also N is fixed at 0.5, the d influence is exhibited (with higher T_s resulting from larger d values), and the $K = 1$ vertical slice represents the symmetric case I limit

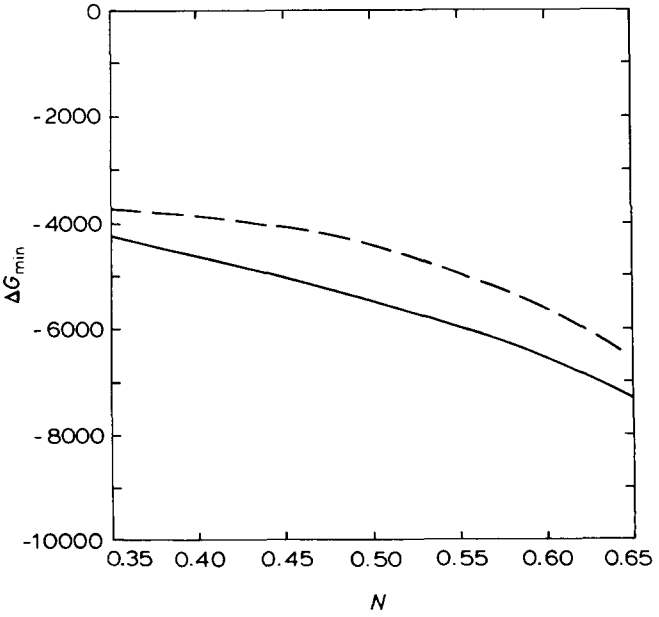

Figure 11 Case IV results are presented for $K = 0.95$; here ΔG_{min} at 373 K is plotted as a function of N for the same SBS triblock used in *Figure 5*. The vertical slice where $N = 0.50$ represents the limit of case III results (for $K = 0.95$ only). Shape factor dependencies are the same as in *Figures 5* and *8*

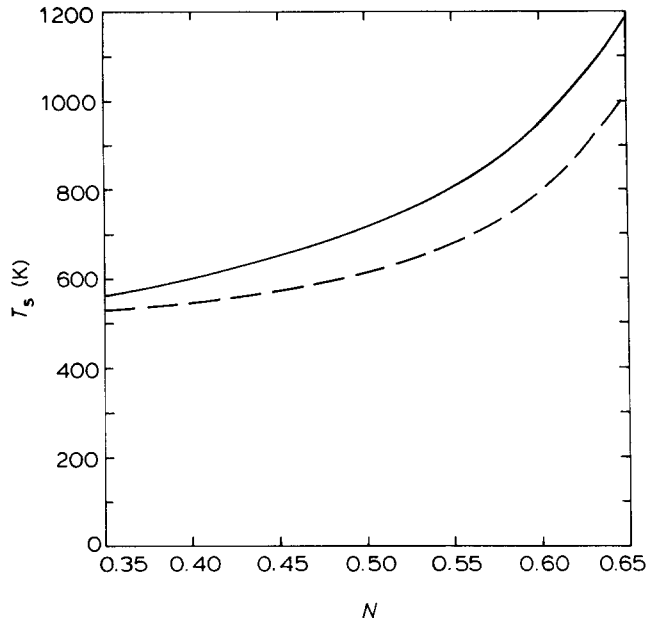

Figure 12 Case IV results for $T_s(N)$ at fixed $K = 0.95$ for the same SBS copolymer as in *Figure 5*, and with d dependencies just as in *Figure 6*. As in *Figure 11*, the $N = 0.50$ results here illustrate the case III limit for $K = 0.95$

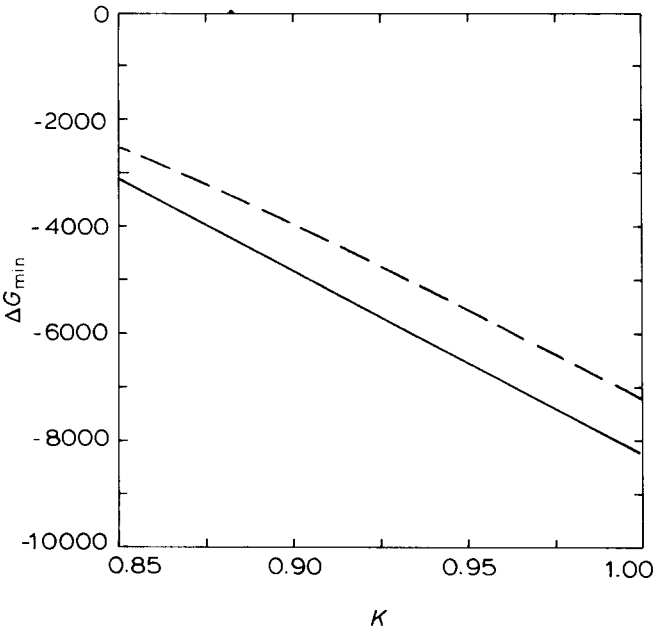

Figure 13 Another slice of the $\Delta G^{373}_{min}(N,K)$ function is exhibited here for $N = 0.60$ and K varying. All calculations are for the same SBS triblock used in *Figure 5*, and shape factor effects are similar to those in *Figure 10*. The vertical slice corresponding to $K = 1$ here encompasses the range of possible case II results for $N = 0.60$

(*Figure 9*), and all qualitative results are the same. In a similar fashion *Figure 14* repeats the qualitative results of *Figure 10* for the $T_s(K,d)$ calculations, only now $N = 0.60$ instead of 0.50.

No further graphical presentations will be included here, though a wide range of calculations have been performed[34]. At no time was a value of ΔG_{min} found which was lower for $\{N, K < 1\}$ than for $\{N, K = 1\}$, nor a T_s which was higher for $\{N, K < 1\}$ than for $\{N, K = 1\}$, for the same value of N.

CONCLUSION

Evidence has been presented for residual mixing of B chains in the A core region of microphase-separated block copolymers. This phenomenon of residual mixing, when coupled with the evidence[20] for asymmetric composition profiles in the interphase region, has resulted in the classification of the four possible cases of symmetry and asymmetry corresponding to all combinations of $\{N = 0.50, N \neq 0.50\}$ and $\{K = 1, K \neq 1\}$.

The recently revised version[9] of the Leary–Williams thermodynamic model for block copolymers has been extended to allow for the cases when $K \neq 1$ (residual mixing in the A core), and calculations have been performed for the various asymmetric cases. This is believed to be the first investigation into the possible effects of such asymmetries on block copolymer properties.

A preference for $N > 0.50$ is seen in the plots of $\Delta G_{min}(N)$, in qualitative agreement with most experimental results[20]. However, the lowest ΔG_{min} was not a true minimum, being found at the largest value of N allowed by a class of polynomial profiles employed for calculations. Because no bounded value for ΔG_{min} was found, no quantitative predictions for the equilibrium values of N are currently available.

Calculations show that ΔG_{min} is not lowered by the introduction of residual mixing for any type of asymmetry considered here. Thus, residual mixing should not be expected when the block copolymer system is at equilibrium. Nature apparently prefers $K = 1$ to the alternative. This conclusion leads to the important inference that the experimentally observed residual mixing ($K < 1$) in some block copolymers must originate from samples that are not, in fact, at equilibrium.

Whether such non-equilibrium morphologies are inevitable (due to severe kinetic limitations or thermodynamic force barriers to morphological transformations) remains to be seen. The definitive experiments would be to measure $\phi'_A(x)$ or K in the melt state, well

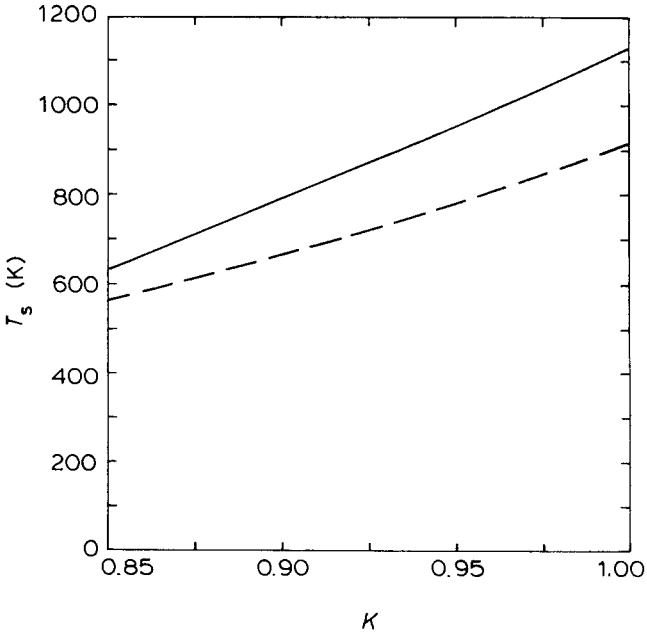

Figure 14 Case IV results for $T_s(K)$ at $N = 0.60$ using the same SBS copolymer as in *Figure 5*. The effects of varying d are the same as before, and the $K = 1$ limit here presents a subset of results for case II (at $N = 0.60$)

above the T_g of the highest-T_g component (where both phases are fluid, have greater chain mobility and a greater likelihood of reaching the equilibrium morphology). In principle, samples should be annealed as close to T_s as possible; a knowledge of T_s is therefore essential for estimating the probability that a given sample treatment has of achieving an equilibrium state. Similar experiments near T_s should be performed to measure $\overline{\phi'_A}$ (or N); this may be easier than measuring K, and is almost certainly easier than obtaining $\phi'_A(x)$.

Finally, a comment should be made on extensions of the theory to include in ΔG a term characterizing long-range intermolecular forces. Such a term, which involves the square of composition gradients in the interphase[5,35], can be introduced into equation (5) so that the multiplier of f becomes

$$\frac{1}{\Delta T}\int_0^{\Delta T}\left[\phi'_A\phi'_B+\frac{t^2}{6}\left(\frac{d\phi'_A}{dx}\right)\right]dx \qquad (23)$$

where t is the Debye interaction range parameter. Calculations have been performed using equation (23) for numerous cases that incorporate symmetrical $\phi'_A(x)$ functions[36], and results are generally insensitive to the new term. For example, using $t=6$ Å (as proposed by Meier[5]) with the $\cos^2$ profile leads to only a 4% increase in equation (23). When applied to the case of an SB copolymer with styrene content $\phi_A=0.25$ and $\tilde{V}=10^5$ cm^3 mol^{-1}, at 298 K, this gives only a 1% change in ΔG_{min} (less negative) and a 4% change in ΔT (1.4 Å larger); the corresponding change in T_s is also about 1% (7 K larger). Results for other $\phi'_A(x)$ profiles are very similar, even when gradients are steep in portions of the interphase. In view of these minor effects in the symmetrical case, together with uncertainties[35] in the value of t and possible additional influences in ΔS (discussed by de Gennes[37]), there is little incentive to inject the gradient term into calculations directed here toward asymmetry influences. Its inclusion would be unlikely to lead to significant changes in most cases.

ACKNOWLEDGEMENT

This work was supported in part by the National Science Foundation, Grant DMR 76-83679, and in part by the Director, Office of Energy Research, Office of Basic Energy Sciences, Materials Science Division of the U.S. Department of Energy under Contract No. DE-AC03-76SF0098.

APPENDIX

CHAIN PLACEMENT IN DOMAINS WITH RESIDUAL MIXING

By definition of the postulated microstructure used previously, the presence of a block junction within an interphase means that the attached A and B chains will reside only in their respective domains (or core regions plus the interphase itself). However, the question of block location re-emerges if a junction is permitted to reside inside a core region, as in this work. It is argued below that all of *both* blocks attached to such a junction (residing in a core region) should be contained totally inside the same core.

Consider a chain occupying the various configurations depicted in *Figure A1* for diblocks or *Figure A2* for triblocks. Whenever there is a local gradient in composition ($d\phi_A/dx$, as occurs in the interphase but not in the core regions), then a chain in that environment is expected[19] to be exposed to a force proportional to $d\phi_A/dx$ (really $d\mu/dx$, where μ is the local chemical potential). This force tends to pull the A chains back toward the A core (and *vice versa* for B chains). Since there is no gradient force inside the core(s), the only net force of this type arises from the interphase contribution.

As a consequence, the positions 1 and 3 illustrated in *Figure A1* are predicted to be unstable—they will be drawn into positions 2 and 4, respectively. Similarly, *Figure A2* illustrates stable and unstable configurations for a triblock. Position 1 is unstable and will convert to position 2. Both positions 3 and 5 in *Figure A2* are unstable and should eventually be drawn into a configuration similar to that in position 4.

So, at any given instantaneous sampling for large numbers of configurations—or for any long-time average—the cases where the block junctions reside in the core but part of the attached blocks do not (as in the odd-

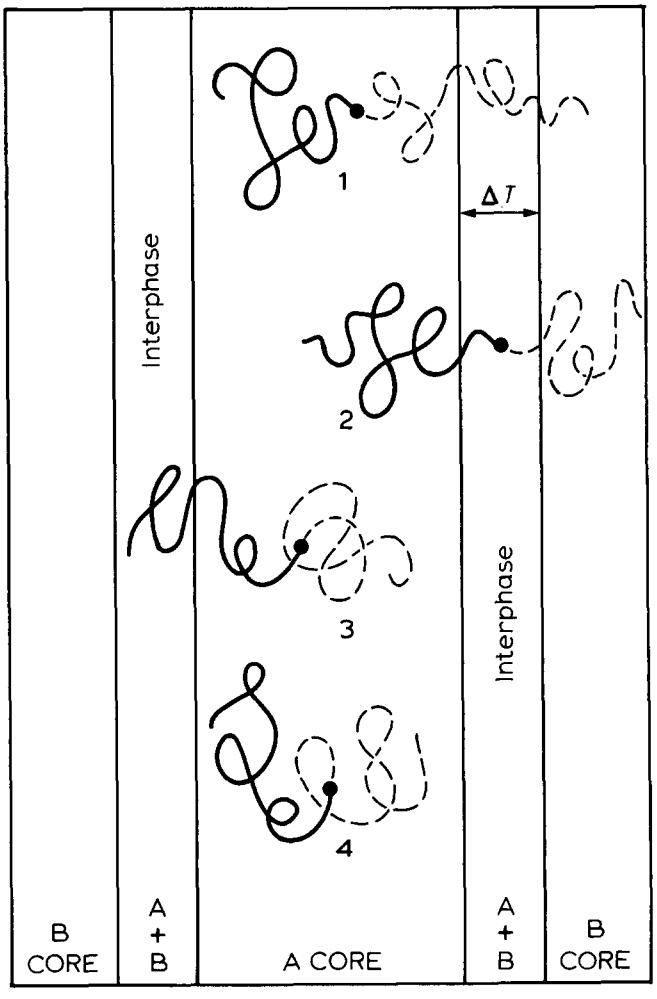

Figure A1 Schematic illustration of possible stable and unstable chain configurations for diblock copolymers whose junctions are allowed to exist in the A core as well as in the interphase (odd-numbered configurations are expected to be unstable, while even-numbered ones are expected to be stable). For AB molecules, the A block is designated by (———) and the B block by (– – –). (●): block junctions

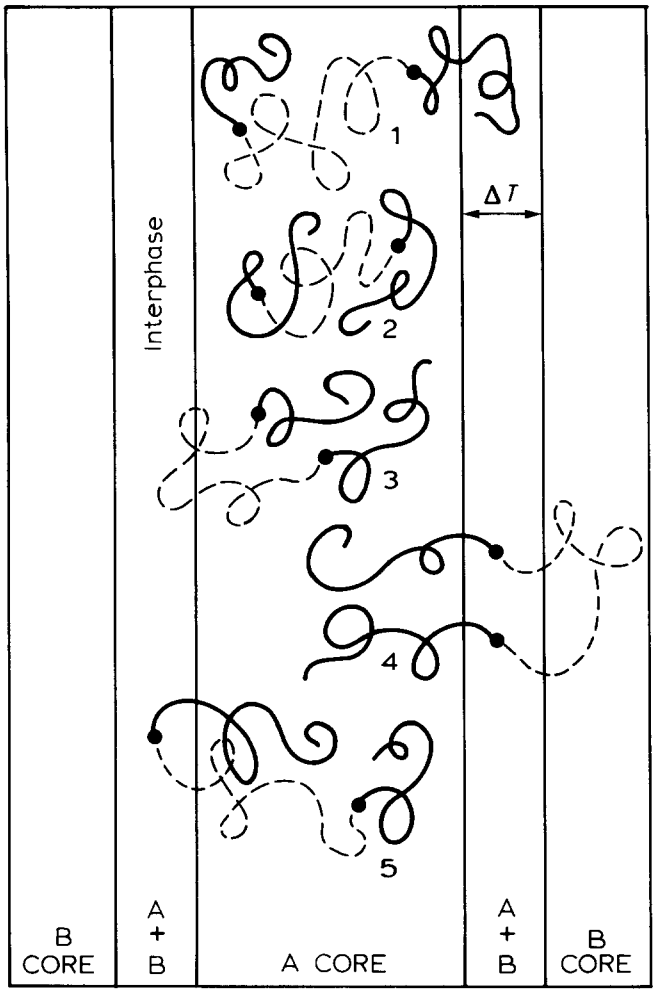

Figure A2 Schematic illustrations of possible unstable configurations (represented by odd-numbered positions) and stable (even-numbered) configurations for a triblock copolymer whose junctions are allowed to be in the A core region in addition to the interphase. For ABA molecules, A blocks are designated by (———) and the B block by (– – –). (●): block junctions

numbered positions in the two Figures) are expected to be a very small percentage of the total number in the existing chain distribution. Hence the assumption that the fraction of junctions inside the A core equals the fraction of B chains entirely inside the A core (used to evaluate ψ in terms of material balance parameters) is expected to be a very good approximation.

REFERENCES

1 Meier, D. J. *J. Polym. Sci., Part C* 1969, **26**, 81
2 Krause, S. *J. Polym. Sci., Part A-2* 1969, **7**, 249; *Macromolecules* 1970, **3**, 84
3 Leary, D. F. and Williams, M. C. *J. Polym. Sci., Polym. Lett. Edn.* 1970, **8**, 335; *J. Polym. Sci., Polym. Phys. Edn.* 1973, **11**, 345; 1974, **12**, 265
4 Meier, D. J. in 'Block and Graft Copolymers', (Eds. J. J. Burke and V. Weiss), Syracuse University Press, New York, USA, 1973, Chap. 6
5 Meier, D. J. *ACS Polym. Prepr.* 1974, **15**(1), 171; Proc. Polymer Colloqium, Kyoto, Japan, Sep. 1977
6 Helfand, E. *Macromolecules* 1975, **8**, 552; Helfand, E. and Wasserman, Z. R. *Macromolecules* 1976, **9**, 879; 1978, **11**, 960; 1980, **13**, 994; *Polym. Eng. Sci.* 1977, **8**, 582
7 Noolandi, J. and Hong, K. M. *Macromolecules* 1982, **15**, 482
8 Cahn, J. W. and Hilliard, J. E. *J. Chem. Phys.* 1958, **28**, 258
9 Henderson, C. P. and Williams, M. C. *J. Polym. Sci., Polym. Phys. Edn. 1985*, **23**, 1001; preliminary results were also presented in *ACS Polym. Prepr.* 1980, **21**(2), 249 and at IUPAC Macromolecular Symposium, Amherst, Mass., USA, 1982
10 Diamant, J., Soong, D. S. and Williams, M. C. in 'Contemporary Topics in Polymer Science', (Ed. W. J. Bailey), Vol. 4, Plenum Press, New York, USA, 1984; see also Polym. Eng. Sci. 1982, **22**, 673 for blends of blocks, and Diamant, J. *Ph.D. Thesis*, University of California, Berkeley, USA, 1982
11 Sivashinsky, N., Moon, T. J. and Soong, D. S. *J. Macromol. Sci., Phys.* 1983, **B22**, 213; Sivashinsky, N. and Soong, D. S. *J. Polym. Sci., Polym. Lett. Edn.* 1983, **21**, 459; Soong, D. S., Sivashinsky, N. and Kelterborn, J. C. *J. Elast. Plast.* 1983, **15**, 193
12 Utracki, L. A. and Kamal, M. R. *Polym. Eng. Sci.* 1982, **22**, 96
13 Hansen, P. J., Hugenberger, G. S. and Williams, M. C., presented at IUPAC Macromolecular Symposium, Amherst, Mass., USA, July 1982; Hansen, P. J. and Williams, M. C., Proc. of SPE National Technical Conference, Bal Harbour, Florida, USA, Oct. 1982; see also Hansen, P. J., M.S. Thesis, University of California, Berkeley, USA, 1982, and Hugenberger, G. S., M.S. Thesis, University of California, Berkeley, USA, 1982
14 Watanabe, H. and Kotaka, T. *Macromolecules* 1983, **16**, 1783; *Polym. J.* 1982, **14**, 739
15 Chen, Y.-D. and Cohen, R. E. *J. Appl. Polym. Sci.* 1977, **21**, 629
16 Annighofer, F. and Gronski, W. *Colloid Polym. Sci.* 1983, **261**, 15; Stadler, R. and Gronski, W. *Colloid Polym. Sci.* 1983, **261**, 215; 1984, **262**, 466
17 Fesko, D. G. and Tschoegl, N. W. *Intern. J. Polym. Mater.* 1974, **3**, 51
18 Kraus, G. and Rollmann, K. W. *J. Polym. Sci., Polym. Phys. Edn.* 1976, **14**, 1133
19 Henderson, C. P. and Williams, M. C. *J. Polym. Sci., Polym. Lett. Edn.* 1979, **17**, 257
20 Henderson, C. P. and Williams, M. C. *Polymer* 1985, **26**, 2021
21 Several authors have made this suggestion; see for example Morese-Seguela, B., St.-Jacques, M., Renaud, J. M. and Prud'homme, J. *Macromolecules* 1980, **13**, 100
22 Krause, S. and Iskandar, M. in 'Multiphase Polymers', Adv. Chem. Series No. 176, (Eds. S. L. Cooper and G. M. Estes), Am. Chem. Soc., Washington, D.C., USA, 1979, p. 205
23 Turner, D. T. *Polymer* 1978, **19**, 789; see also Glans, J. H. and Turner, D. T. *Polymer* 1981, **22**, 1540
24 Couchman, P. R. *J. Polym. Sci., Polym. Phys. Edn.* 1977, **15**, 1037; *J. Polym. Sci., Polym. Symp.* 1978, **63**, 271
25 Bares, J. *Macromolecules* 1975, **8**, 244
26 Bywater, S. *Polym. Eng. Sci.* 1984, **24**, 104
27 Zurawski, D. E. and Sperling, L. H. *Polym. Eng. Sci.* 1983, **23**, 510
28 Krause, S. and Iskander, M. *J. Polym. Sci., Polym. Phys. Edn.* 1981, **19**, 1659
29 Krause, S., Lu, Z-h. and Iskandar, M. *Macromolecules* 1982, **15**, 1076
30 Brown, I. M. *Macromolecules* 1981, **14**, 801
31 Bergmann, K. and Gerberding, K. *Colloid Polym. Sci.* 1981, **259**, 990
32 Hobbs, S. Y. and Watkins, V. H. *J. Polym. Sci., Polym. Phys. Edn.* 1982, **20**, 651
33 See e.g., Somani, R. H. and Shaw, M. T. *Polym. Eng. Sci.* 1984, **24**, 601
34 Henderson, C. P. *Ph.D. Thesis*, Univ. of California, Berkeley, USA, 1985
35 McMaster, L. T. in 'Copolymers, Polyblends and Composites', Adv. Chem. Series No. 142, (Ed. N. A. J. Platzer), Am. Chem. Soc., Washington, D.C., USA, 1975, p. 43
36 Spontak, R. J., unpublished calculations for Ph.D. thesis in progress, University of California, Berkeley, USA, 1984
37 De Gennes, P.-G. *J. Chem. Phys.* 1980, **72**, 4756

NOMENCLATURE

a,b,c Coefficients of the polynomial profile, defined in terms of d, K and N
A Refers to component A in an AB diblock or ABA triblock; by convention, the A component is the higher-T_g material
AB Notation for a diblock copolymer
ABA Notation for a triblock copolymer
B Refers to component B in an AB diblock or ABA triblock

d The adjustable shape parameter in the polynomial profile

f Volume fraction of the interphase material present in the planar morphology

f_{AC} Volume fraction of the A core material present in the planar morphology

D The planar morphology repeat distance (as defined in *Figure 1*)

G Molar Gibbs free energy of a block copolymer; subscripts 'struc' and 'homog' refer to the structured (microphase-separated) and the homogeneous reference states, respectively

ΔG The free energy difference between the microphase-separated morphology and the reference homogeneous morphology at the same temperature

ΔH Enthalpy change upon going from the homogeneous reference state to the microphase-separated morphology

K The volume fraction of component A in the A core region or, equivalently, the value of the interphase composition profile at $x = \Delta T$ (the A-core edge)

K_i Chain expansion parameter relating molecular weight to end-to-end distances for homopolymer species i

N The volume average of component A in the interphase region

PB Notation for polybutadiene homopolymer or block

PS Notation for polystyrene homopolymer or block

P_i Chain probability function for component i (where i = A or B)

R Universal gas constant

ΔS Entropy change upon going from the homogeneous reference state to the microphase-separated morphology

ΔS_i The contribution to ΔS associated with restricting the i block to the i domain (the T_i region), where i = A or B

ΔS_1 That contribution to ΔS associated with restricting the junction to reside in an interphase

$\Delta S_j^{(K)}$ The formulation that results for the entropy term j (here j = A, B or 1) in the 'new' configurations, when K is allowed to be less than unity

$\Delta S_j^{(1)}$ The formulation for entropy term j (here j = A, B or 1) for those chains in the 'old' or K = 1 positions

T Temperature

T_i Domain size of component i in planar morphology; in magnitude it contains an i core region and the two adjacent interphases

T_s The separation temperature; above T_s the morphology is homogeneous, below T_s the morphology is microphase-separated

T_g^i Glass transition temperature of component i, where i = A or B

$\tilde{V}$ The total molar volume of the block copolymer (for densities near unity, the magnitude of $\tilde{V}$ is very close to that of the molecular weight)

$\langle r_i^2 \rangle$ The actual end-to-end distance squared of block i

$\langle r_i^2 \rangle_0$ The unperturbed end-to-end distance squared of block i, assumed to equal the end-to-end distance squared of homopolymer i

x A position variable across the interphase region; in magnitude it ranges from 0 to ΔT

Greek symbols

α_i The ratio of the actual to the unperturbed end-to-end distance for block i

β The dimensionless interphase thickness—one of two model parameters (in the thermodynamic theory) which are varied to minimize the free energy

β_{min} That value of β which is found to correspond to the minimum value of the free energy

Γ The dimensionless A-domain size—one of two model parameters (in the thermodynamic theory) which are varied to minimize the free energy

Γ_{min} That value of Γ which is found to correspond to the minimum value of the free energy

δ_i The value of the solubility parameter of block i, presumed to equal the value for homopolymer i

ε A small increment in position across the interphase

ϕ_i The volume fraction of component i in the block copolymer molecule

$\phi_i'(x)$ The local volume fraction of component i across the interphase, as a function of position x

$\overline{\phi_i'}$ The volume average of component i in the interphase

$\overline{\phi_A' \phi_B'}$ The volume average of the product of the two local volume fractions across the interphase region

ρ_i The mass density of component i, assumed to be equal to the density of homopolymer i

μ The local value of the chemical potential

ψ The fraction of all block copolymer junctions that are located in the A core